

## Structural and Optical Properties of E)-3-(benzylideneamino)-5-ethyl-6-(hydroxymethyl)-2-(methoxymethyl)-2,3,4,5,6-Pentamethyltetrahydro-2H- pyran-4-ol

Hajer Abusnina<sup>\*1,2</sup>, N. A. El-Ghamaz<sup>1</sup> and E. A. Gaml<sup>1</sup>

<sup>1</sup>Department of Physics, Faculty of Science, Damietta University 34517, Egypt.

<sup>2</sup>High and Intermediate Institute of Agricultural Technology-Gheran. Tripoli, Libya.

Received: 10 January 2025 /Accepted: 09 February 2025

\*Corresponding author's E-mail: [hajer.gege2014@gmail.com](mailto:hajer.gege2014@gmail.com)

### Abstract

A new polymer was synthesized based on the Chitosan polymer. The structural and optical properties of the Chitosan derivative thin films have been investigated. The X-ray diffraction (XRD) measurements showed that the powder is amorphous for CH-BHM. The thermal stability of CH-M derived polymer was investigated using TGA measurements. TGA analysis showed that polymer was stable from room temperature up to 373 K. The optical properties of thin films were investigated using the spectrophotometric measurements. The absorption spectrum and The absorption coefficient,  $\alpha$ , were determined. The values of the optical energy gap  $E_g$  of the compound under test was found to be 5.24 eV. A quantitative study concerning the localized states in the forbidden gap (Urbach tail) was performed.

**Keywords:** Chitosan derivative; Thermal stability; Optical absorption; Energy gap.

### Introduction

Owing to their exceptional and tunable properties, organic materials have garnered significant research interest for their potential applications in numerous technological domains including optical devices (M. N. V. R. Kumar et al., 2004; Pillai et al., 2009). Research efforts are concentrated on developing novel materials based on conducting polymers and their derivatives, aiming for high stability, good

conductivity, and significant energy storage capability while maintaining cost effectiveness (Natsumeda et al., 1977). Optical features such as band gap energy is inherent to these polymers due to the abundance of  $\pi$ -electron delocalization along their backbones (Chiang et al., 1978). Chitosan is a Chitin derivative known for its biocompatible, biodegradable, and non-toxic nature (Morgado et al., 2013). Chitosan and its derivatives have garnered significant attention owing to their antimicrobial and antifungal properties (Muzzarelli et al., 1986; Qi et al., 2004).

Chitosan has the most abundant natural amino polysaccharide after cellulose with special structure, multidimensional properties, and various applications in biomedical and other industrial areas (Hirano, 1996). Applications based on the optical properties of Chitosan and its derivatives are emerging and growing. For instance, the development of sensors to detect metal ions and biological structures, based on resonant excitation of surface free-electrons oscillations has been considered (Sugunan et al., 2005).

In the present work, we aimed to investigate structural, thermal stability and optical absorption properties of one of the chitosan derivative, namely, E)-3-(benzylideneamino)-5-ethyl-6-(hydroxymethyl)-2-(methoxymethyl)-2,3,4,5,6-pentamethyltetrahydro-2H- pyran-4-ol.

## Experimental techniques

### Material

In this work, a novel polymer was derived from Chitosan as start material. The derived polymer is: E)-3-(benzylideneamino)-5-ethyl-6-(hydroxymethyl)-2-(methoxymethyl)-2,3,4,5,6-pentamethyltetrahydro-2H- pyran-4-ol (CH-BHM). The chemical structure of the derived polymer is depicted in Fig 1. The derivative CH-BHM has been synthesized according to the method present by (Diab et al., 2011).

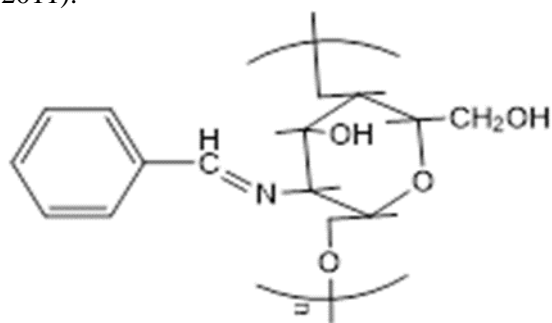


Fig.1: The molecular structural of CH-BHM.

### Measurements and Characterization Samples preparation

In the present work The XRD measurements of polymers powder was performed using (Shimadzu XRD 6000) in the range  $4 - 8^\circ$ , with step of 0.01 degrees per second with Cu  $K\alpha$  radiation source

(wavelength of  $0.15406 \text{ \AA}$ ), generator voltage of 40 KV. The TGA measurements were performed using a TG-50 instrument from Shimadzu (Japan) for testing the thermal behavior of samples. The heating was carried out at temperature range from room temperature up to  $500^\circ\text{C}$  with a heating rate of  $10^\circ\text{C}/\text{min}$  under nitrogen gas atmosphere. The nitrogen flow was kept at a constant rate of about 20 mL/min. Finally, the absorption measurements recorded by JASCO model V-630 in the range 200-900 nm for samples in the form of thin film. In practice, CH-BHM is insoluble in organic solvents. To overcome this issue, 0.3 g of the mixtures of pure Chitosan and CH-BHM with ratio 2:1 in 8 mL acetic acid solution and 4 ml distilled water for 12h to ensure complete dissolving and mixing to produce **Chi-1** which is suitable for thin film preparation by spin coating technique. Thin film was prepared by spin coating technique onto quartz substrates using VTC-50A Spin Coater at 1500 rpm for coating and 2500 rpm for drying for 30 s.

## Result and discussion

### Structural analysis

#### X-ray diffraction

The X-ray diffraction patterns (XRD) for CH-BHM is shown in Fig 2. This figure confirms the amorphous phase of CH-BHM. The obtained XRD pattern is demonstrating the same behavior of most polymers (S. Kumar & Koh, 2012).

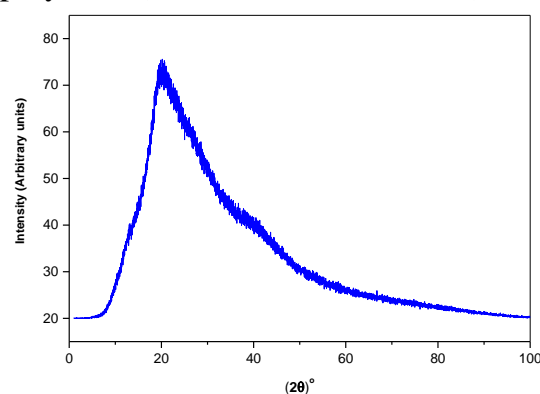


Fig 2: XRD patterns of CH-BHM

### Thermal Analysis

Figure 3 presents the thermogravimetric analyses (TGA) thermogram and its derivative with respect to temperature (DTG) for CH-BHM in the temperature range 28-490 °C. In the first stage, the heating up to 80 °C, the CH-BHM loses about 15% of its weight. This loss can be attributed to the loss of humidity and/or solvents residuals. The maximum loss rate appeared at about 56 °C as shown in the DTG curve. CH-BHM appeared to be thermally stable in the range 115-205 °C. At the temperature range 205-490 °C, the polymer continues to lose weight with a high loss rate. The maximum loss rate appeared at 287 °C as determined by the second peak of the DTG curve. Such behavior may be attributed to the degradation by loss of phenyl group (Osman & Arof, 2003; Țucureanu et al., 2016) and the continuous degradation of the backbone of the polymer.

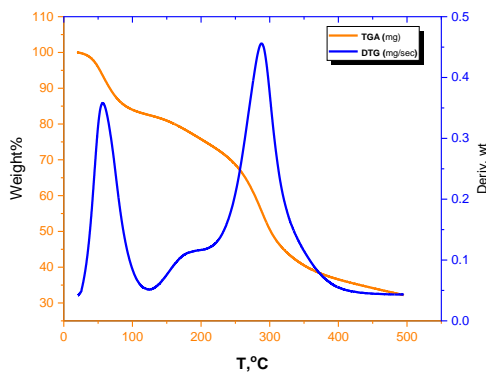


Fig 3: Thermal Analysis (TGA & DTG) of CH-BHM

### Optical characterization

#### Absorption characteristics and Energy gap:

The absorption spectrum provides valuable insights into the band structure of materials. The absorption coefficient ( $\alpha$ ) of the material thin film can be determined from experimentally measured absorbance data using Equation (1) (Hassanien et al., 2020):

$$\alpha = 2.303 \frac{A}{d} \quad (1)$$

where  $A$  and  $d$  are the absorbance and thickness of thin film, respectively. Figs. 4 and 5 show the measured Absorbance and the calculated values of  $\alpha$  for Ch-1 thin film as a function of  $\lambda$ . It is clear that the absorption coefficient ( $\alpha$ ) has values greater than  $1 \times 10^3$  cm<sup>-1</sup>. As well, there is absorption peak

appeared at  $\lambda \approx 291$  nm and 355 nm in the UV-region of spectrum. These two peaks may be attributed to  $\pi$ - $\pi^*$  orbital transition from bonding to antibonding molecular orbitals (Baerends et al., 2002)

Determining the energy gap ( $E_g$ ) and identifying the nature of electron transitions are crucial for effectively utilizing materials in device fabrication. To this end, we determined  $E_g$  and the type of electron transitions by analyzing the optical absorption near the absorption edge. We employed the following relationship proposed by (Baerends et al., 2002) to analyze the absorption coefficient ( $\alpha$ ) in this region.

$$\alpha h\nu = B(h\nu - E_g)^r, \quad (2)$$

In Equation (2),  $B$  represents a constant that is related to both electrical conductivity and the energy level separation. The parameter ' $r$ ' characterizes the nature of the electronic transition. For direct transitions, ' $r$ ' assumes values of 1/2 for allowed transitions and 3/2 for forbidden transitions. In the case of indirect transitions, ' $r$ ' takes on values of 2 for allowed transitions and 3 for forbidden transitions (Baerends et al., 2002). By differentiating Equation (2) with respect to photon energy ( $h\nu$ ) and then dividing Equation (2) by this derivative, we obtain the following relation:

$$\left[ \frac{\alpha h\nu}{d(\alpha h\nu)/d(h\nu)} \right] = \frac{1}{r} (h\nu - E_g). \quad (3)$$

A plot of  $\alpha h\nu / (d(\alpha h\nu) / d(h\nu))$  versus  $h\nu$  is a straight line in the spectral range near the absorption edge with a slope of  $1/r$  of about 0.5 and so the best expected type of electronic transition is indirect allowed. The values of the optical band gap ( $E_g$ ) and onset gap ( $E_{\text{onset}}$ ) energies for chi-1 is determined by extrapolating the linear portion of the absorption edge to the x-axis, as shown in Figure 6, and are determined to be 5.24, 2.26 eV, respectively.

Amorphous semiconductors and insulators, like polymers, often exhibit localized states within their bandgaps. In general, localized states are energy levels within the bandgap of a semiconductor that trap electrons, preventing them from freely moving and contributing to electrical conduction. These localized states near the band gap edge can be characterized quantitatively using the Urbach relation (Urbach, 1953):

$$\alpha = \alpha_o \exp\left(\frac{h\nu}{E_u}\right) \quad (4)$$

where  $\alpha_o$  is a constant and  $E_u$  represents the extent of these states within the band gap. Understanding the extent of these states is crucial for optimizing the performance of devices fabricated from this polymer, such as organic solar cells or electronic devices. By analyzing the relationship between the absorption coefficient and the incident photon energy for the polymer thin film under investigation as depicted in Figure 7, the values of  $E_u$  is directly the reciprocal of the slope. The value of  $E_u$  is calculated and found to be 0.35 eV.

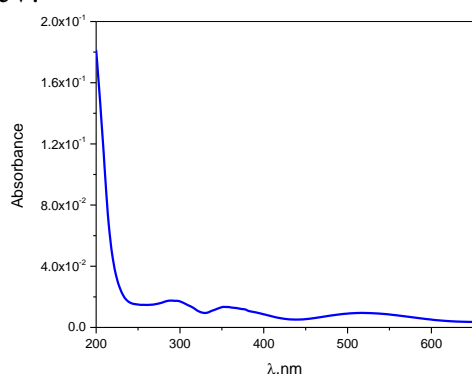


Fig 4: Absorbance spectrum of Chi-1 thin film

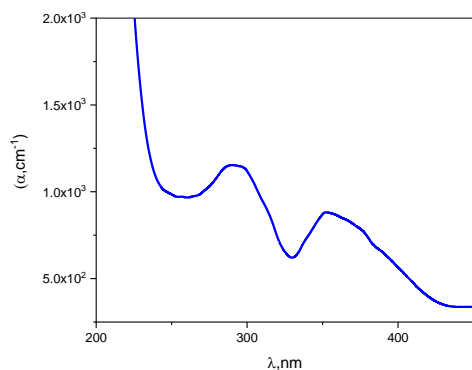


Fig 5: Absorption coefficient  $\alpha$  for Chi-1 thin film

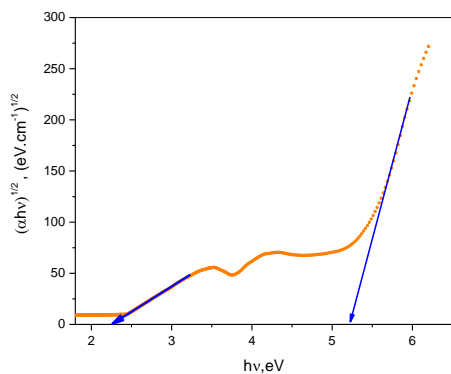


Fig 6 : Dependence of  $(\alpha h\nu)^{1/2}$  on  $h\nu$  for Chi-1

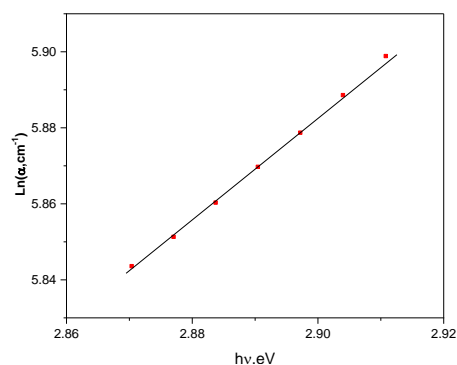


Fig 7: Plot of  $\text{Ln } \alpha$  versus incident photon energy,  $h\nu$ , for Chi-1 thin film

## Conclusion

The present study, E)-3-(benzylideneamino)-5-ethyl-6-(hydroxymethyl)-2-(methoxymethyl)-2,3,4,5,6- pentamethyltetrahydro-2H- pyran-4-ol. (CH-BHM) is derived from Chitosan. The amorphous nature of CH-BHM is confirmed by XRD. Also the thermal analysis by thermogravimetric analysis (TGA) revealed that CH-BHM is thermally stable at temperature up to 205 °C while it is under degradation with the more increase of temperature. CH-BHM is found to be insoluble. For studying the optical properties, a mixture of CH-BHM and Chitosan is successfully prepared, and spin coated onto quartz substrates. The electronic transitions are found in the UV region of spectra and attributed to the  $\pi$ - $\pi^*$  transition from bonding to antibonding molecular orbitals. The type of electronic transition near the absorption edge is found to be indirect forbidden and values of fundamental and onset energy gaps is found to be 5.24, 2.26 eV, respectively.

## References

- Baerends, E. J., Ricciardi, G., Rosa, A., & Van Gisbergen, S. J. A. (2002). A DFT/TDDFT interpretation of the ground and excited states of porphyrin and porphyrazine complexes. *Coordination Chemistry Reviews*, 230(1–2), 5–27. [https://doi.org/10.1016/S0010-8545\(02\)00093-0](https://doi.org/10.1016/S0010-8545(02)00093-0)
- Chiang, C. K., Druy, M. A., Gau, S. C., Heeger, A. J., Louis, E. J., MacDiarmid, A. G., Park, Y. W., & Shirakawa, H. (1978). Synthesis of highly conducting films of derivatives of polyacetylene, (CH)<sub>x</sub>. *Journal of the American Chemical Society*, 100(3), 1013–1015. <https://doi.org/10.1021/ja00471a081>

- Diab, M. A., El-Sonbati, A. Z., & Bader, D. M. D. (2011). Thermal stability and degradation of chitosan modified by benzophenone. *Spectrochimica Acta Part A: Molecular and Biomolecular Spectroscopy*, 79(5), 1057–1062. <https://doi.org/10.1016/j.saa.2011.04.019>
- Hassanien, A. S., El Radaf, I. M., & Akl, A. A. (2020). Physical and optical studies of the novel non-crystalline  $Cu_xGe_{20-x}Se_{40}Te_{40}$  bulk glasses and thin films. *Journal of Alloys and Compounds*, 849, 156718. <https://doi.org/10.1016/j.jallcom.2020.156718>
- Hirano, S. (1996). Chitin Biotechnology Applications. In *Biotechnology Annual Review* (Vol. 2, pp. 237–258). Elsevier. [https://doi.org/10.1016/S1387-2656\(08\)70012-7](https://doi.org/10.1016/S1387-2656(08)70012-7)
- Kumar, M. N. V. R., Muzzarelli, R. A. A., Muzzarelli, C., Sashiwa, H., & Domb, A. J. (2004). Chitosan Chemistry and Pharmaceutical Perspectives. *Chemical Reviews*, 104(12), 6017–6084. <https://doi.org/10.1021/cr030441b>
- Kumar, S., & Koh, J. (2012). Physiochemical, Optical and Biological Activity of Chitosan-Chromone Derivative for Biomedical Applications. *International Journal of Molecular Sciences*, 13(5), 6102–6116. <https://doi.org/10.3390/ijms13056102>
- Morgado, J., Pereira, A. T., Braganca, A. M., Ferreira, Q., Fernandes, S. C. M., Freire, C. S. R., Silvestre, A. J. D., Pascoal Neto, C., & Alcacer, L. (2013). Self-standing chitosan films as dielectrics in organic thin-film transistors. *Express Polymer Letters*, 7(12), 960–965. <https://doi.org/10.3144/expresspolymlett.2013.94>
- Muzzarelli, R., Jeuniaux, C., & Gooday, G. W. (Eds.). (1986). *Chitin in Nature and Technology*. Springer US. <https://doi.org/10.1007/978-1-4613-2167-5>
- Natsumeda, Y., Yoshino, M., & Tsushima, K. (1977). Hypoxanthine-guanine phosphoribosyltransferase from rat liver. Effects of magnesium 5-phosphoribosyl 1-pyrophosphate on the chemical modification and stability of the enzyme. *Biochimica Et Biophysica Acta*, 483(1), 63–69. [https://doi.org/10.1016/0005-2744\(77\)90008-0](https://doi.org/10.1016/0005-2744(77)90008-0)
- Osman, Z., & Arof, A. K. (2003). FTIR studies of chitosan acetate based polymer electrolytes. *Electrochimica Acta*, 48(8), 993–999. [https://doi.org/10.1016/S0013-4686\(02\)00812-5](https://doi.org/10.1016/S0013-4686(02)00812-5)
- Pillai, C. K. S., Paul, W., & Sharma, C. P. (2009). Chitin and chitosan polymers: Chemistry, solubility and fiber formation. *Progress in Polymer Science*, 34(7), 641–678. <https://doi.org/10.1016/j.progpolymsci.2009.04.001>
- Qi, L., Xu, Z., Jiang, X., Hu, C., & Zou, X. (2004). Preparation and antibacterial activity of chitosan nanoparticles. *Carbohydrate Research*, 339(16), 2693–2700. <https://doi.org/10.1016/j.carres.2004.09.007>
- Sugunan, A., Thanachayanont, C., Dutta, J., & Hilborn, J. G. (2005). Heavy-metal ion sensors using chitosan-capped gold nanoparticles. *Science and Technology of Advanced Materials*, 6(3–4), 335–340. <https://doi.org/10.1016/j.stam.2005.03.007>
- Țucureanu, V., Matei, A., & Avram, A. M. (2016). FTIR Spectroscopy for Carbon Family Study. *Critical Reviews in Analytical Chemistry*, 46(6), 502–520. <https://doi.org/10.1080/10408347.2016.1157013>
- Urbach, F. (1953). The Long-Wavelength Edge of Photographic Sensitivity and of the Electronic Absorption of Solids. *Physical Review*, 92(5), 1324–1324. <https://doi.org/10.1103/PhysRev.92.1324>

## الملخص العربي

**عنوان البحث:** الخصائص البنيوية والبصرية لـ E)-3-(بنزليدينامينو)-5-إيثيل-6-(هيدروكسي ميثيل)-2-(ميثوكسي ميثيل)-3,4,5,6-بنتاميثيليترا هيدرو-2 بييران-4-أول

هاجر عاشور محمد أبوسنيّة<sup>1\*</sup>، ناصر عبده عبدالرازق الغماز<sup>1</sup>، إيمان أسعد جمل<sup>1</sup>

<sup>1</sup>قسم الفيزياء – كلية العلوم – جامعة دمياط – مصر.

خلال الدراسة الحالية تم تحضير المركب العضوي (CH-BHM) المشتقة من الكيتوزان. تم تأكيد الطبيعة غير المتبلورة للبوليمر بواسطة تقنية حيود الأشعة السينية وكذلك كشف التحليل الحراري باستخدام التحليل الحراري الكتلتي (TGA) أن CH-BHM مستقر حرارياً عند درجة حرارة تصل إلى 200 درجة مئوية بينما يخضع للتحلل مع زيادة درجة الحرارة أكثر من ذلك. وجد أن CH-BHM غير قابل للذوبان في المذيبات العضوية مما صعب الحصول منه على أغشية رقيقة مناسبة لدراسة الخصائص البصرية. تم تحضير خليط من CH-BHM والكيتوزان (Chi-1) بنجاح وتم تحضير أغشية رقيقة منه على ركائز من الكوارتز

باستخدام تقنية الطلاء المغزلي . تم تحديد الانتقالات الإلكترونية في منطقة الأشعة فوق البنفسجية من الطيف وعزيت إلى انتقال  $\pi-\pi^*$  من المدارات الجزيئية الرابطة إلى المدارات الجزيئية المضادة للرابطة. كما تم تحديد نوع الانتقال الإلكتروني بالقرب من حافة الامتصاص حيث تبين أنه من النوع غير المباشر وكذلك تم حساب قيم فجوات الطاقة الأساسية وبداية الامتصاص حيث كانت  $2.26$  ،  $5.24$  إلكترون فولت على التوالي.